

# Automating UbiFast for High-throughput and Multiplexed Ubiquitin Enrichment

## Authors

Keith D. Rivera, Meagan E. Olive, Erik J. Bergstrom, Alissa J. Nelson, Kimberly A. Lee, Shankha Satpathy, Steven A. Carr, and Namrata D. Udeshi

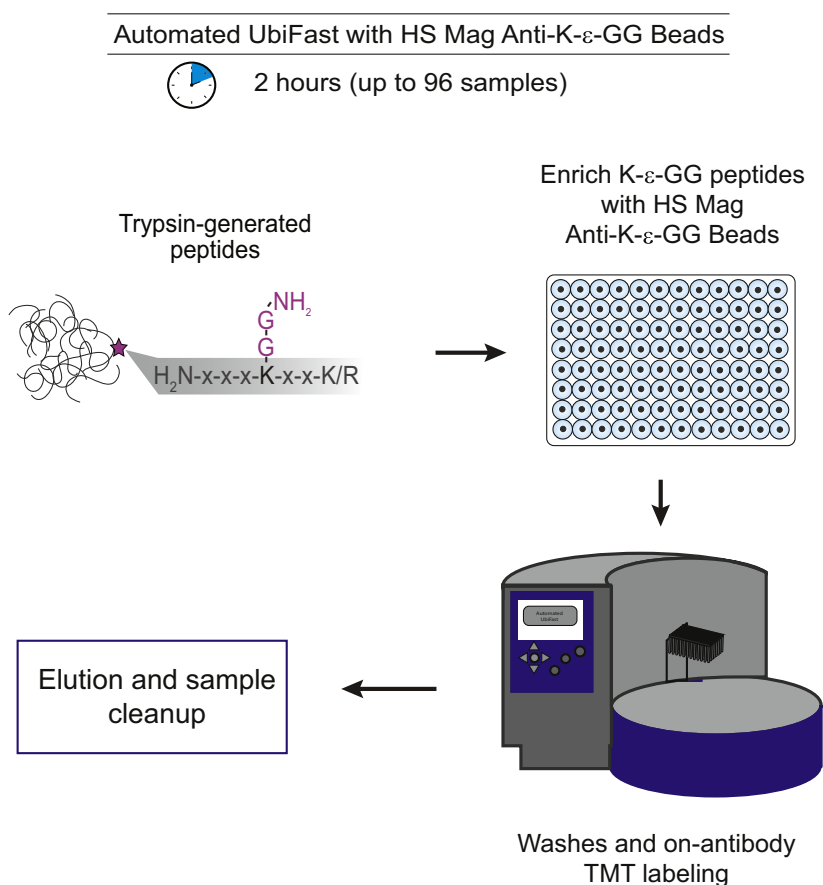
## Correspondence

scarr@broad.mit.edu; udeshi@broadinstitute.org

## In Brief

We present automation of the UbiFast method using a magnetic bead-conjugated K- $\epsilon$ -GG antibody and a magnetic particle processor. We report the identification of ~20,000 ubiquitylation sites from a TMT10-plex with 500  $\mu$ g input per sample in ~2 h. Automation of the UbiFast method greatly increased the number of identified and quantified ubiquitylation sites, improved reproducibility, and significantly reduced processing time. The workflow enables processing of up to 96 samples in a single day making it suitable to study ubiquitylation in large sample sets.

## Graphical Abstract



## Highlights

- HS mag anti-K- $\epsilon$ -GG antibody increases sensitivity of ubiquitylation site detection.
- Automated UbiFast increases reproducibility and sample processing throughput.
- The automated UbiFast workflow enables processing of up to 96 samples in one day.
- UbiFast can be employed to profile ubiquitylomes from small amounts of tumor tissue.



# Automating UbiFast for High-throughput and Multiplexed Ubiquitin Enrichment

Keith D. Rivera<sup>1</sup>, Meagan E. Olive<sup>1</sup>, Erik J. Bergstrom<sup>1</sup>, Alissa J. Nelson<sup>2</sup>, Kimberly A. Lee<sup>2</sup>, Shankha Satpathy<sup>1</sup>, Steven A. Carr<sup>1,\*</sup>, and Namrata D. Udeshi<sup>1,\*</sup>

**Robust methods for deep-scale enrichment and site-specific identification of ubiquitylation sites are necessary for characterizing the myriad roles of protein ubiquitylation. To this end we previously developed UbiFast, a sensitive method for highly multiplexed ubiquitylation profiling where K- $\epsilon$ -GG peptides are enriched with anti-K- $\epsilon$ -GG antibody and labeled on-antibody with isobaric labeling reagents for sample multiplexing. Here, we present robotic automation of the UbiFast method using a magnetic bead-conjugated K- $\epsilon$ -GG antibody (mK- $\epsilon$ -GG) and a magnetic particle processor. We report the identification of ~20,000 ubiquitylation sites from a TMT10-plex with 500  $\mu$ g input per sample processed in ~2 h. Automation of the UbiFast method greatly increased the number of identified and quantified ubiquitylation sites, improved reproducibility, and significantly reduced processing time. The automated method also significantly reduced variability across process replicates compared with the manual method. The workflow enables processing of up to 96 samples in a single day making it suitable to study ubiquitylation in large sample sets. Here we demonstrate the applicability of the method to profile small amounts of tissue using breast cancer patient-derived xenograft (PDX) tissue samples.**

Ubiquitylation is a highly conserved protein post-translational modification regulating a wide variety of cellular functions including regulation of protein turnover through the ubiquitin-proteasome system (1). The ubiquitylation process is regulated by E1 activating, E2 conjugating, E3 ligating enzymes together with deubiquitinases (2, 3). Dysregulation of ubiquitylation enzymes and deubiquitinases can lead to aberrant activation or deactivation of pathways involved in many disease processes, notably cancer progression, neurodegeneration, and innate and adaptive immune regulation (4). Drugs targeting the ubiquitin system such as proteasome inhibitors have proven highly successful in the clinic (5, 6). The development of additional therapeutics targeting this pathway

is emerging but remains highly dependent on continued understanding of ubiquitination biology in disease (7–9).

Liquid chromatography–tandem mass spectrometry (LC-MS/MS) is the leading method for unbiased analysis of protein modifications, including protein ubiquitylation (10, 11). Analysis of ubiquitylated proteins is typically carried out by first using trypsin to generate peptides suitable for LC-MS/MS analysis. Trypsin cleaves proteins at the carboxyl side of lysine (Lys) and arginine (Arg). When ubiquitin is attached to a substrate protein, trypsin digestion leaves a glycine–glycine (GG) remnant on the side chain of Lys residues of tryptic peptides, which were formerly ubiquitylated. Antibodies that recognize this di-glycyl remnant (K- $\epsilon$ -GG) are used to enrich ubiquitylated (Ub) peptides for analysis by LC-MS/MS (12–15).

Isobaric chemical tags such as the Tandem Mass Tag (TMT) system are commonly used to compare up to 18 samples within a single experiment and provide precise relative quantitation of peptides and proteins (16–19). A major limitation of integrating TMT quantitation and ubiquitylation profiling with K- $\epsilon$ -GG antibodies is that these antibodies no longer recognize and enrich peptides when the N-terminus of the di-glycyl remnant is derivatized with TMT. To overcome this limitation, we recently developed the UbiFast method for highly sensitive and multiplexed analysis of ubiquitylation sites from cells or tissue (20). The UbiFast method employs an anti-K- $\epsilon$ -GG antibody for enrichment of K- $\epsilon$ -GG peptides followed by on-antibody TMT labeling. Specifically, K- $\epsilon$ -GG peptides are labeled with TMT reagents while still bound to the anti-K- $\epsilon$ -GG antibody, allowing the NHS-ester group of the TMT reagent to react with the peptide N-terminal amine group and the  $\epsilon$ -amine groups of lysine residues, but not the primary amine of the di-glycyl remnant. Subsequently, TMT-labeled K- $\epsilon$ -GG peptides from each sample are combined while still on bead, eluted from the antibody, and analyzed by LC-MS/MS. The UbiFast approach eliminates cell culture restrictions, greatly reducing the amount of input material required relative to

From the <sup>1</sup>Broad Institute of MIT and Harvard, Cambridge, Massachusetts, USA; <sup>2</sup>Cell Signaling Technology, Danvers, Massachusetts, USA  
Data availability

The original mass spectra and the protein sequence database used for searches have been deposited in the public proteomics repository MassIVE (<http://massive.ucsd.edu>) and are accessible at <ftp://massive.ucsd.edu/MSV000087363/>.

\*For correspondence: Namrata D. Udeshi, [udeshi@broadinstitute.org](mailto:udeshi@broadinstitute.org); Steven A. Carr, [scarr@broad.mit.edu](mailto:scarr@broad.mit.edu).

SILAC-based experiments (12, 13, 21–27) and improves Ub-peptide recovery and analysis time compared with in-solution TMT labeling strategies (28). The sensitivity of the UbiFast method makes it suitable for studies in primary tissue samples.

Although the UbiFast method is highly effective for deep-scale LC-MS/MS analysis of ubiquitylated peptides, the throughput is limited because all workflow steps are manually executed, making the procedure somewhat laborious. In addition, an initial cross-linking step is necessary to covalently couple the anti-K- $\epsilon$ -GG antibody to agarose beads, to prevent contamination of enriched samples with antibody (13). Furthermore, slight variations during the K- $\epsilon$ -GG peptide enrichment processing steps can result in an increased variability across replicates within a given TMT experiment.

To improve the UbiFast method we have now evaluated and optimized use of a commercially available anti-K- $\epsilon$ -GG antibody supplied irreversibly coupled to magnetic beads (HS mag anti-K- $\epsilon$ -GG). We demonstrate that HS mag anti-K- $\epsilon$ -GG antibody enables automation of the UbiFast method on a magnetic bead processor, greatly increasing sample processing throughput while reducing variability across experimental replicates. We also show that automation of the UbiFast method can be easily scaled to process multiple TMT experiments in just a few hours. The automated UbiFast method was benchmarked against the previously published, manually executed UbiFast method for profiling patient-derived breast cancer xenograft tissue. Surprisingly, we found that the automated magnetic-bead method also significantly increased the depth of coverage of the ubiquitylome.

### EXPERIMENTAL PROCEDURES

#### *In-Solution Digestion of Jurkat Cell Lysates*

Jurkat cells were grown in suspension with RPMI 1640 medium, glutaMAX supplement (Life Technologies), and 10% heat-inactivated fetal bovine serum (Life Technologies). Cells were pelleted, washed 2 $\times$  with 1 $\times$  PBS (pH 7.4), and lysed. Lysis buffer consisted of 8 M urea, 50 mM tris hydrochloride (Tris-HCl) pH 8.0, 150 mM sodium chloride (NaCl), and 1 mM ethylenediaminetetraacetic acid (EDTA). Immediately before lysing, the following additives were added to their respective final concentrations: aprotinin (Sigma) to 2  $\mu$ g/ml, leupeptin (Roche) to 10  $\mu$ g/ml, phenylmethylsulfonyl fluoride (PMSF) (Sigma) to 1 mM, PR-619 (LifeSensors) to 50  $\mu$ M, and chloroacetamide (CAA) to 1 mM. Cells were lysed for 30 min on ice and then centrifuged for 10 min at 20,000g and 4  $^{\circ}$ C. Protein concentration was then determined using a bicinchoninic acid (BCA) assay kit (Thermo Fisher Scientific). The lysate was diluted to 8 mg/ml with lysis buffer, dithiothreitol (DTT) was added to a final concentration of 5 mM, and it was incubated at room temperature (RT) for 45 min. Next, iodoacetamide (IAA) was added to a final concentration of 10 mM, and the lysate was incubated for 30 min at RT in the dark. Then the lysate was diluted 1:4 with 50 mM Tris-HCl, pH 8.0. After dilution Lys-C (Wako) was added with an enzyme to substrate ratio of 1:50, and the lysate was incubated for 2 h at RT. Trypsin was then added with an enzyme to substrate 1:50, and the lysate was incubated overnight at RT. The following morning neat formic acid (FA)

was added to a final concentration of 1%, and the sample was centrifuged for 10 min at 10,000g to remove urea and undigested proteins. Peptides were cleaned up using a 500 mg Sep-Pak tC18 solid-phase extraction cartridge (Waters). Briefly, the cartridge was conditioned with 5 ml of Acetonitrile (ACN)/0.1% FA and then 50% ACN/0.1% FA. Equilibration was performed with four additions of 5 ml 0.1% trifluoroacetic acid (TFA). Digested peptides were loaded and then washed twice with 5 ml 0.1% TFA. Peptides were eluted with two additions of 50% ACN/0.1% FA. The eluate was frozen at  $-80^{\circ}$ C and dried to completion *in vacuo*. Peptides were reconstituted in 30% ACN/0.1% FA, and peptide concentration was measured using a BCA assay kit. The peptides were divided into 500  $\mu$ g aliquots, frozen at  $-80^{\circ}$ C, and dried in vacuum. Once dried the peptide aliquots were stored at  $-80^{\circ}$ C until use.

#### *Label-Free Comparison of Manual Immunoprecipitation With Agarose Versus Magnetic Beads*

Agarose beads used in all antibody comparisons were from the PTMScan Ubiquitin Remnant Motif (K- $\epsilon$ -GG) Kit (Cell Signaling Technology, Kit #5562). Preparation of agarose beads included cross-linking as described previously (20). All agarose bead washes were performed with immunoprecipitation (IAP) buffer (50 mM MOPS, pH 7.2, 10 mM sodium phosphate, 50 mM NaCl). Magnetic beads for all experiments come from PTMScan HS Ubiquitin/SUMO Remnant Motif (K- $\epsilon$ -GG) Kit (Cell Signaling Technology, Kit #59322), along with 1 $\times$  HS IAP Bind Buffer #1 and 1 $\times$  HS IAP Wash Buffer. Magnetic beads were used as provided, with no additional cross-linking. Input for manual comparisons was 500  $\mu$ g digested Jurkat peptide, and enrichments were performed in triplicate.

Jurkat samples were reconstituted with 1.5 ml of either IAP buffer for agarose-bead IPs or 1 $\times$  HS IAP Bind Buffer #1 for magnetic-bead IPs. Reconstituted peptides were confirmed to be pH 7 and were spun at 10,000g for 5 min (pH adjusted with 1 M Tris if necessary). After cross-linking, agarose beads were suspended in a slurry of 1:25 beads to IAP buffer from which 62.5  $\mu$ l slurry (31.25  $\mu$ g antibody) was used per IP. Magnetic beads are provided in a 20% slurry, and enough was removed for a given experiment to be washed 3 $\times$  with 1 ml ice-cold 1 $\times$  PBS, inverted  $\sim$ 5 $\times$  with each wash, and resuspended again in original volume. Different magnetic bead amounts were tested for this label-free comparison, including 10  $\mu$ l slurry (2  $\mu$ l beads) and 5  $\mu$ l slurry (1  $\mu$ l beads) per IP. Beads were aliquoted into clean 1.5 ml snap-cap Eppendorf tubes.

Reconstituted peptides were added to aliquoted antibody beads and incubated at 4  $^{\circ}$ C for 1 h, gently rotating end-over-end. Buffers were chilled during this enrichment step, and all remaining wash steps were performed on ice when tubes were not being handled. After incubation, agarose beads were centrifuged at 2000g for 1 min and allowed to settle for  $\sim$ 10 s before removing supernatant as IP flow-through. Simultaneously, magnetic beads were spun at 2000g for 5 s and allowed to settle for  $\sim$ 10 s on a magnetic rack before slowly removing flow-through. Sample flow-throughs can be stored at  $-80^{\circ}$ C for serial analyses.

All washes were performed as quickly as possible. For agarose bead IPs, beads were washed 4 $\times$  with 1.5 ml PBS, inverting  $\sim$ 5 $\times$  with each wash, centrifuging at 2000g for 1 min, letting beads settle, and aspirating supernatant. Magnetic beads were washed 4 $\times$  with 1 ml 1 $\times$  HS IAP Wash Buffer and 2 $\times$  with 1 ml HPLC H<sub>2</sub>O, inverting  $\sim$ 5 $\times$  with each wash, centrifuging for  $\sim$ 5 s at 2000g, and allowing beads to be drawn to magnet for  $\sim$ 10 s before aspirating supernatant. Ubiquitin peptides were eluted from all beads with 50  $\mu$ l 0.15% TFA for 10 min at RT, gently flicking the beads into solution every 2–3 min. While eluting, 2-punch Empore C18 (3M) StageTips were conditioned and equilibrated 1 $\times$  with 100  $\mu$ l methanol (MeOH), 1 $\times$  with 100  $\mu$ l 50% ACN/0.1% FA, and 2 $\times$  with 1% FA.

Upon completion of the first elution, samples were centrifuged quickly at 2000g, placed on a magnetic rack where applicable, and the supernatant containing ubiquitin peptides was loaded onto its designated conditioned StageTip. The elution step was repeated and the supernatant similarly loaded onto the StageTip to be washed 2x with 100  $\mu$ l 1% FA and eluted with 50  $\mu$ l 50% ACN/0.1% FA. Desalted eluates were transferred to HPLC vials, frozen at  $-80^{\circ}\text{C}$ , and dried *via* vacuum centrifugation.

Samples were reconstituted in 9  $\mu$ l 3% ACN/0.1% FA and 4  $\mu$ l was analyzed *via* nanoflow liquid chromatography coupled to tandem mass spectrometry, or LC-MS/MS, using an Easy-nLC 1200 system (Thermo Fisher Scientific) online with a Q-Exactive HF-X mass spectrometer (Thermo Fisher Scientific). Samples were injected and chromatographically separated on a fused silica microcapillary column (360  $\mu$ m OD  $\times$  75  $\mu$ m ID) with a 10  $\mu$ m electrospray emitter tip (New Objective) packed to  $\sim$ 25 cm with ReproSil-Pur 1.9  $\mu$ m C18-AQ beads (Dr Maisch GmbH) and heated to  $50^{\circ}\text{C}$ . Online separation occurred over a 154 min gradient, employing a changing ratio of solvent A (3% ACN/0.1% FA) to solvent B (90% ACN/0.1% FA). Gradient steps as min:% solvent B include 0:2, 2:6, 122:35, 130:60, 133:90, 143:90, 144:50, 154:50, starting at a mobile phase flow rate of 200 nl/min for the first six steps and increasing to 500 nl/min for the final two.

Ion acquisition was performed with a data-dependent analysis method. MS1 scans were collected across a range of 300–1800 m/z at a resolution of 60,000, with an automatic gain control (AGC) target of 3E6 ions and maximum injection time of 10 ms. Within a scan, the top 20 most abundant peaks were picked for higher-energy collisional dissociation (HCD) fragmentation using a collision energy of 28 and isolation window of 0.7 m/z. MS2 spectra were acquired in centroid mode at a resolution of 45,000 with an AGC target of 1E5 and maximum injection time of 150 ms. Peptide matching was set to “preferred,” dynamic exclusion was 20 s, and ions with unassigned charge or charge =1 or >7 were excluded.

#### *Comparison of TMT Labeling Efficiency With Agarose Versus Magnetic Beads*

A comparison of TMT labeling efficiency of K- $\epsilon$ -GG peptides captured by agarose *versus* magnetic antibody beads was done in triplicate, using 500  $\mu$ g Jurkat peptide input. Beads were aliquoted as described above, using 62.5  $\mu$ l agarose slurry and 5  $\mu$ l magnetic slurry per IP. Sample reconstitution, incubation with antibody, and flow-through collection were performed exactly as outlined above. Samples enriched with agarose or magnetic beads were washed once with 1 ml IAP buffer or 1x HS IAP Wash buffer and once with 1 ml 1x PBS or HPLC H<sub>2</sub>O, respectively. With each wash, samples were inverted approximately five times, centrifuged at 2000g for  $\sim$ 5 s, and allowed to settle on ice or a magnetic rack before aspirating the supernatant.

After washing and immediately before labeling, all beads were resuspended in 200  $\mu$ l 100 mM HEPES (pH 8.5). Each sample was labeled with a single TMT channel (126C, 127N, 127C for agarose replicates and 128N, 128C, 129N for magnetic replicates), adding 400  $\mu$ g reagent in 10  $\mu$ l anhydrous ACN directly to the resuspended beads. Tubes were shaken at 1400 rpm for 10 min at RT. Labeling was then quenched with 8  $\mu$ l 5% hydroxylamine followed by 5 additional minutes of shaking at 1400 rpm at RT. Excess reagent was washed away 1x with 1.3 ml and 2x with 1.5 ml respective IAP wash buffers, inverting tubes approximately five times, centrifuging for  $\sim$ 5 s at 2000g, and allowing beads to settle before removing the supernatant. Beads were similarly washed 2x with 1.5 ml 1x PBS (agarose) or HPLC H<sub>2</sub>O (magnetic) before eluting and stage tipping exactly as described above.

Samples were analyzed similarly to the previous label-free experiment, with the reconstitution and liquid chromatography method being identical. Data acquisition was performed using an Orbitrap

Exploris 480 mass spectrometer (Thermo Fisher Scientific) with a data-dependent analysis method. MS1 parameters were the same as above, with the exception of a 100% normalized AGC target. A precursor fit filter was employed, with a fit threshold of 50% and window of 1.4 m/z. MS2 spectra were collected with an HCD collision energy of 32%, resolution of 15,000, AGC target of 50%, and maximum injection time of 120 ms. Remaining ion acquisition parameters were the same as previously described.

#### *Developing Enrichment of K- $\epsilon$ -GG Peptides Using the KingFisher Flex*

For all optimization enrichments, 500  $\mu$ g of dried Jurkat peptides was reconstituted in 250  $\mu$ l PTMScan HS IAP Bind Buffer #1 with a final concentration of 0.01% CHAPS and placed in a sonicator bath for 2 min pH was confirmed to be neutral, and then solution was cleared by centrifugation for 5 min at 10,000g. Magnetic beads from PTMScan HS Ubiquitin/SUMO Remnant Motif (K- $\epsilon$ -GG) Kit were prepared as described above. After washing beads 3x with ice cold 1x PBS, beads were reconstituted to their original volume with HS IAP Bind Buffer #1, and beads were aliquoted into individual wells of a 200  $\mu$ l, 96 well KingFisher plate (Thermo Fisher Scientific). The solution of cleared peptides was added to the wells containing beads, the plate was covered with aluminum sealing film (Axygen) and rotated end-over-end for 1 h at  $4^{\circ}\text{C}$ , except where otherwise noted.

In order to determine if CHAPS is a necessary addition to buffers when using the KF, we processed triplicate ubiquitin enrichments with all buffers containing either 0.01% CHAPS or all buffers without CHAPS added. To assess the feasibility of performing the K- $\epsilon$ -GG peptide capture step on the KF, enrichments were done in triplicate on the KingFisher for 1 h at room temperature with medium mixing. Separately, duplicate enrichments were done in 96-well KingFisher plates offline with end-over-end rotating in a cold room at  $4^{\circ}\text{C}$ . The wash buffer used for these experiments was HS IAP Wash Buffer with a final concentration of 0.01% CHAPS.

To test the viability of using lower volumes of beads, 5  $\mu$ l, 10  $\mu$ l, and 20  $\mu$ l of slurry were processed in quintuplicate using the label-free KingFisher Flex method described below. Each replicate was injected separately onto the mass spectrometer.

In the interest of assessing the optimal wash buffer, HS IAP Wash Buffer with 0.01% CHAPS was compared with a modified version of this buffer where it was diluted 1:1 with ACN to make 50% ACN, 50% HS IAP Wash Buffer with 0.005% CHAPS.

For label-free experiments a six-step KingFisher Flex method was used. Step 1 collects the beads from the incubation plate containing the Jurkat peptides and the magnetic beads. For comparisons where incubation of peptides and beads is performed on the KingFisher Flex, this step mixes the plate at medium speed for 1 h. For experiments where the capture of K- $\epsilon$ -GG peptides occurs offline, this step mixes the plate at medium speed for 30 s and then collects the beads. Steps 2 through 4 are 1 min washes with 250  $\mu$ l of washing buffer where the first 15 s are on the bottom mix setting and the remaining 45 s are set to fast mixing. Step 5 is a wash for 1 min with 250  $\mu$ l of HPLC water with medium mixing. The final step is elution in 100  $\mu$ l of 0.15% TFA for 10 min with slow mixing. For all steps a collect count of 5 and collection time of 1 s was used. The eluted peptides were then cleaned up using the stage-tip protocol described above. Similarly, these samples were chromatographically separated and injected onto an Orbitrap Exploris 480 using the same methods described above.

#### *Comparison of Full TMT10 Plex Experiments Manual Versus Automated*

To evaluate the performance of the automated UbiFast protocol compared with the manual UbiFast protocol using the same PTMScan HS magnetic bead kit, we designed three parallel isobaric labeling

experiments using TMT10 reagent. For each experiment there were ten process replicates, where each process replicate was 500 µg of dried Jurkat peptides. One of these experiments was performed using the UbiFast protocol (20). The other two experiments were performed on the optimized automated UbiFast protocol described below. These experiments were identical except one labeled with the TMT10 reagent for 10 min and the other labeled with TMT10 reagent for 20 min to assess the effect of increased labeling time on labeling efficiency.

For all three experiments, the desalted sample was transferred to an HPLC vial, frozen, and dried *via* vacuum centrifugation. Dried peptides were then reconstituted in 9 µl 3% ACN/0.1% FA and analyzed with back-to-back injections of 4 µl using the same liquid chromatography parameters as above. Ion acquisition was performed with an Orbitrap Exploris 480 (Thermo Fisher Scientific) mass spectrometer in line with a FAIMS Pro Interface (Thermo Fisher Scientific). The FAIMS device was operated in standard resolution mode at 100 °C, utilizing the compensation voltages (CVs) of -40, -60, and -80 for the first injection followed by a second injection with CVs of -40, -50, and -70. Remaining parameters were identical to the previous manual TMT-labeling comparison experiment, with the exceptions of utilizing a top ten method for MS2 spectra collection and an MS2 resolution of 45,000.

### *UbiFast Protocol Using HS Mag Anti-K-ε-GG Reagent*

For the manual UbiFast comparison, a 10-plex experiment with 500 µg Jurkat peptide input per channel was performed. Five microliters magnetic beads were washed and aliquoted into ten 1.5 ml tubes, and K-ε-GG peptide enrichment was performed as described above. After IP, flow-throughs were collected and saved, all samples were washed with 1 ml 1× HS IAP Wash Buffer followed by 1 ml HPLC H<sub>2</sub>O, inverting approximately five times before centrifuging for ~5 s at 2000g and removing the supernatant on a magnetic rack. TMT labeling and quenching were performed identically to the previous single channel experiment, using a full TMT10 10-plex. Samples were washed first with 1.3 ml followed by 1.5 ml 1× HS IAP Wash Buffer. After washing, each of the ten TMT-labeled samples was individually resuspended in 90 µl 1× HS IAP Wash Buffer and combined while still bound to bead into a single 1.5 ml tube. This combined sample was mixed by inverting approximately five times and concentrated by spinning in a benchtop centrifuge at 2000g for 5–10 s. Beads were allowed to settle on a magnetic rack and the supernatant was slowly aspirated. The ten original IP tubes were serially washed with 1.5 ml 1× HS IAP Wash Buffer to collect any remaining beads, and this wash was added to the final sample. Two washes with 1.5 ml HPLC water were performed before eluting TMT-labeled K-ε-GG peptides with 150 µl 0.15% TFA for 10 min at RT, tapping the tube every 2–3 min to resuspend the beads. The eluate was collected by spinning the sample briefly, setting the tube in a magnetic rack, and slowly pipetting the supernatant onto a StageTip preconditioned as described above. This elution step was repeated once, and the sample was StageTip desalted in a manner identical to previous experiments.

### *Optimized Automated UbiFast Protocol Using HS Mag Anti-K-ε-GG Reagent*

The automated UbiFast experiments were performed as follows: 5 µl of magnetic bead slurry was aliquoted into ten wells of a 96-well KingFisher plate. 500 µg of dried Jurkat peptides were reconstituted in 250 µl of HS IAP Bind Buffer with 0.01% CHAPS, placed in a bath sonicator for 2 min and clarified by centrifugation for 5 min at 10,000g. The peptide solution was then pipetted into individual wells in a 96-well KF plate containing HS mag anti-K-ε-GG. The plate was covered with aluminum sealing film (Axygen) and rotated end-over-end for 1 h at 4 °C.

The plate containing peptides and HS mag anti-K-ε-GG was then moved to the KF. Immediately prior to beginning the method on the KF, 400 µg of TMT reagent in 10 µl ACN was pipetted into corresponding wells of a 96-well KF plate. Then 190 µl of 100 mM HEPES was added to the TMT containing wells. The KF method for TMT labeling consists of seven steps. Step 1 collects the beads from the incubation plate containing the Jurkat peptides and the magnetic beads after mixing at medium speed for 30 s. Step 2 washes the beads with 250 µl of modified HS IAP Wash Buffer [50% ACN/50% HS IAP Wash Buffer with 0.01% CHAPS] for 1 min. Step 3 washes the beads with 250 µl of 1× PBS with 0.01% CHAPS for 1 min. Step 4 is on-antibody TMT labeling with 400 µg of TMT reagent per channel and either 10 or 20 min of labeling time. Step 5 is quenching with 250 µl of 2% hydroxylamine for 2 min. Step 6 is a final wash with 250 µl of the modified HS IAP Buffer for 1 min. The final step of the KingFisher Flex protocol is to mix the beads in 100 µl of 1× PBS for 1 min and then the beads are left in the PBS. For all steps the mixing for the first 15 s of the step is set to bottom mix and the remaining time is set to fast. Also, a collect count of 5 and collection time of 1 s were used for all steps. The peptides in PBS were then combined and transferred to a 1.7 ml Eppendorf tube and placed on a magnetic rack for 10 s. The PBS was removed and 100 µl of 0.15% TFA was added to the beads. This elution was repeated once more and both eluates were loaded onto a stage-tip as described previously.

### *Evaluation of Running Multiple Automated UbiFast Experiments Simultaneously*

To evaluate increased throughput by automatically and simultaneously enriching multiple TMT plexes, 40 replicates of 500 µg dried peptides were enriched for K-ε-GG and labeled as 4 × TMT10 plexes. All steps were carried out in parallel, using the optimized automated UbiFast workflow described above. Briefly, 5 µl of PBS-washed HS mag anti-K-ε-GG bead slurry was aliquoted into 4 × 10 adjacent wells of a 96-well KF plate. Dried 500 µg aliquots of A375 melanoma cell line peptides were each reconstituted in 250 µl of HS IAP Bind Buffer with 0.01% CHAPS, vortexed and shook at 1200 rpm for 5 min, and clarified by centrifugation for 5 min at 10,000g. The peptide solutions were then pipetted into each well containing the magnetic bead slurry. The plate was covered with aluminum film and rotated end-over-end for 1 h at 4 °C. After incubation the plate was processed on the KF where washing, on-antibody TMT labeling, and collection of beads in PBS occurred. Each set of K-ε-GG enriched peptides was combined by TMT10 plex into 1.7 ml Eppendorf tubes and placed in a magnetic rack for 10 s. The PBS was removed and 100 µl 0.15% TFA was added to the beads to elute. The elution was repeated once and both eluates were loaded onto stage-tips as previously described. Desalted samples were analyzed *via* FAIMS-LC-MS/MS as previously described.

### *Processing and Analysis of Comparative Reference Tissue*

Processing of WHIM2 and WHIM16 patient-derived xenografts (PDX) for ubiquitylome analysis was described previously (20). Briefly, frozen tissue from each model was lysed, digested, and aliquoted into 500 µg aliquots. For this experiment 20–50 mg of xenograft tissue was used to obtain 500 µg of peptide input (29). Five replicates of WHIM2 and five replicates of WHIM16 were included in a single TMT10-plex experiment. The digested tissue was processed using the optimized automated UbiFast protocol, and LC/MS analysis was performed exactly as detailed in the previous section.

### *Data Analysis*

Mass spectrometry data was processed using Spectrum Mill (Rev B1.07.04.210, Agilent Technologies). For all samples, extraction of raw

files retained spectra within a precursor mass range of 600–6000 Da and a minimum MS1 signal-to-noise ratio of 25. MS1 spectra within a retention time range of  $\pm 45$  s, or within a precursor  $m/z$  tolerance of  $\pm 1.4$   $m/z$  were merged. MS/MS searching of Jurkat and A375 cells was performed against a human RefSeq database released September 14, 2016 containing 38,295 entries. MS/MS searching of PDX samples was performed against a human and mouse RefSeq database with a release date of June 29, 2018 and 72,908 entries. Digestion parameters were set to “trypsin allow P” with an allowance of four missed cleavages. The MS/MS search included fixed modification of carbamidomethylation on cysteine. For TMT quantitation experiments TMT10 was searched using the partial-mix function. Variable modifications were acetylation of the protein N-terminus, oxidation of methionine and remnant GG on lysine. Restrictions for matching included a minimum matched peak intensity of 40% and a precursor and product mass tolerance of  $\pm 20$  ppm. Peptide matches were validated using a maximum false discovery rate (FDR) threshold of 1.2%. FDR was calculated by comparing the number of top database hits from a reversed database search to the total number of top hits in the forward database. TMT10 reporter ion intensities were corrected for isotopic impurities in the Spectrum Mill protein/peptide summary module using the aFRICA correction method, which implements determinant calculations according to Cramer's Rule (30).

#### Experimental Design and Statistical Rationale

For the statistical analysis of PDX models, each protein ID was associated with a log<sub>2</sub>-transformed expression ratio for every sample condition over the median of all sample conditions. After median normalization, a two-sample moderated *t* test was performed on the data to compare treatment groups using an internal R-Shiny package based in the limma library. *p*-values associated with every protein were adjusted using the Benjamini–Hochberg FDR approach (31).

## RESULTS

### Comparison of Magnetic- and Agarose-bead Antibody Reagents for Manual Enrichment of K- $\epsilon$ -GG Peptides

The PTMScan HS Ubiquitin/SUMO Remnant Motif (K- $\epsilon$ -GG) Kit (#59322) contains the same monoclonal antibody as the original PTMScan Ubiquitin Remnant (K- $\epsilon$ -GG Kit) (#5562), with the key difference being that in the new kit, the antibody is irreversibly bound to magnetic beads instead of non-covalently bound to agarose. The bind and wash buffers in the kit have also been optimized to maximize sensitivity and specificity of K- $\epsilon$ -GG peptide enrichment. The antibody is coupled to the beads using chemistry that does not affect the epitope binding regions. Since this HS mag anti-K- $\epsilon$ -GG formulation does not require an initial chemical cross-linking step to covalently couple the antibody to affinity beads, 1–2 days of procedural time are saved (13, 28, 32). The magnetic bead formulation also provides the means to transfer ubiquitin enrichment protocols to a magnetic particle processor for automating and increasing the throughput of sample handling steps.

To characterize the performance of HS mag anti-K- $\epsilon$ -GG, the enrichment of K- $\epsilon$ -GG peptides was directly compared with enrichment with agarose-bead anti-K- $\epsilon$ -GG antibody (PTMScan Ubiquitin Remnant Motif (K- $\epsilon$ -GG) Kit) in a label-free manner. Enrichment of K- $\epsilon$ -GG peptides was completed

in triplicate from 500  $\mu$ g of tryptic peptides derived from Jurkat cells using 5  $\mu$ l and 10  $\mu$ l of HS mag anti-K- $\epsilon$ -GG slurry *versus* 8  $\mu$ l of agarose-bead anti-K- $\epsilon$ -GG antibody and enriched peptides were analyzed by LC-MS/MS (supplemental Fig. S1 and supplemental Data S1). Previous work has shown 8  $\mu$ l anti-K- $\epsilon$ -GG agarose-bead reagent to be optimal for enrichment of K- $\epsilon$ -GG peptides (33). An average of 8662 K- $\epsilon$ -GG PSMs were identified with 5  $\mu$ l of HS mag anti-K- $\epsilon$ -GG, 9284 K- $\epsilon$ -GG PSMs were identified with 10  $\mu$ l of HS mag anti-K- $\epsilon$ -GG while 6643 K- $\epsilon$ -GG PSMs were identified with 8  $\mu$ l anti-K- $\epsilon$ -GG agarose-bead antibody. Using 5  $\mu$ l or 10  $\mu$ l of HS mag anti-K- $\epsilon$ -GG improved recovery of K- $\epsilon$ -GG PSMs compared with 8  $\mu$ l anti-K- $\epsilon$ -GG agarose-bead antibody by 30% and 39%, respectively. The percentage of K- $\epsilon$ -GG PSMs identified relative to the total number of PSMs identified in the sample (relative yield) was 51% with 5  $\mu$ l of HS mag anti-K- $\epsilon$ -GG, 57% with 10  $\mu$ l of HS mag anti-K- $\epsilon$ -GG, and 32% with 8  $\mu$ l anti-K- $\epsilon$ -GG agarose-bead antibody. These results show that HS mag anti-K- $\epsilon$ -GG beads outperformed the anti-K- $\epsilon$ -GG agarose-bead antibody reagent, yielding a larger number of K- $\epsilon$ -GG-peptides with greater specificity using as little as 5  $\mu$ l of magnetic beads. Using 10  $\mu$ l of HS mag anti-K- $\epsilon$ -GG beads provided only a relatively small increase in the number of identified K- $\epsilon$ -GG PSMs *versus* the use of 5  $\mu$ l of HS mag anti-K- $\epsilon$ -GG slurry, indicating that the lower amount of beads is efficient and cost-effective. Twenty microliters slurry of HS mag anti-K- $\epsilon$ -GG, the manufacturer's recommended amount per 1 mg sample, was not evaluated in this study.

### Evaluation of On-antibody TMT Labeling Using HS Mag Anti-K- $\epsilon$ -GG

The UbiFast method utilizes on-antibody TMT labeling for isobaric labeling experiments (20). To evaluate the performance of on-antibody TMT labeling using HS mag anti-K- $\epsilon$ -GG antibody, Jurkat peptides (500  $\mu$ g in triplicate) were enriched using HS mag anti-K- $\epsilon$ -GG or agarose-bead anti-K- $\epsilon$ -GG antibody and labeled with TMT reagent as previously described (20) (supplemental Data S2). For this evaluation, a single channel of TMT reagent was used to label each replicate. We identified an average of 8008 and 5289 K- $\epsilon$ -GG PSMs with 5  $\mu$ l magnetic and 8  $\mu$ l agarose-bead antibody reagent, respectively (supplemental Fig. S1B).

To analyze the efficiency of on-antibody TMT labeling, we evaluated the number of K- $\epsilon$ -GG PSMs fully TMT labeled, partially TMT labeled, and unlabeled. A peptide is considered fully labeled if the N-terminal amine group ( $-NH_2$ ) and the  $\epsilon$ -amino group on lysines (if present) have both reacted with the TMT reagent. Partially labeled PSMs have one amine group that has reacted with TMT and at least one amine group that has not reacted with the TMT reagent. For the agarose bead experiments, 91% of the K- $\epsilon$ -GG PSMs were fully labeled and 5% were partially labeled. For the magnetic bead experiments, 91% of the K- $\epsilon$ -GG PSMs were fully labeled and 5% were partially labeled (supplemental Fig. S1C). The

overlap of K- $\epsilon$ -GG sites identified using HS mag anti-K- $\epsilon$ -GG and anti-K- $\epsilon$ -GG antibody was >54% (supplemental Fig. S1D). Each method also identified a subset of distinct K- $\epsilon$ -GG sites. These results demonstrate that on-antibody TMT labeling works effectively with HS mag anti-K- $\epsilon$ -GG and HS mag anti-K- $\epsilon$ -GG outperforms anti-K- $\epsilon$ -GG antibody for identifying K- $\epsilon$ -GG peptides following enrichment and on-antibody TMT labeling.

### Optimization of Automated Workflow for the UbiFast Method

To increase the throughput and reproducibility of the UbiFast method, we sought to reduce the number of manual sample processing steps in the method by automating the HS mag anti-K- $\epsilon$ -GG washing and on-antibody TMT labeling steps using the KingFisher Flex (KF), a magnetic bead processor compatible with use of 96-well plates. The KF operates by using magnetic rods to collect magnetic beads from wells in a 96-well plate and transfers beads into another 96-well plate, following offline K- $\epsilon$ -GG peptide capture with HS mag anti-K- $\epsilon$ -GG antibody beads in a 96-well plate. Following peptides capture, the plate is loaded onto a KF where antibody beads are washed and K- $\epsilon$ -GG peptides are labeled with TMT reagent while still on HS mag anti-K- $\epsilon$ -GG beads (supplemental Fig. S2).

First, we evaluated how efficiently HS mag anti-K- $\epsilon$ -GG antibody beads transfer from one 96-well plate to a second 96-well plate on the KF. Previous work showed that adding low concentrations of CHAPS to buffers prevents magnetic beads from sticking to plates and being lost during KF processing steps (34). Therefore, we compared automation of UbiFast on the KF with and without addition of 0.01% CHAPS to wash buffers. We found that addition of CHAPS to wash buffers significantly improved automated handling of the magnetic beads, identifying 1.9-fold more K- $\epsilon$ -GG peptides compared with no CHAPS addition (3329 versus 1752 K- $\epsilon$ -GG PSMs) (supplemental Fig. S3A and supplemental Data S3). Omitting CHAPS from wash buffers resulted in residual HS mag anti-K- $\epsilon$ -GG beads being left in the plates after the completion of the KF run. These experiments confirmed that CHAPS improves the movement of magnetic beads in this protocol, increasing the number of K- $\epsilon$ -GG PSMs by 89% and decreasing variability due to loss of beads and should be added to all buffers used on the KF platform.

We next tested if capture of K- $\epsilon$ -GG peptides with HS mag anti-K- $\epsilon$ -GG antibody beads could be carried out on the KF. In the manual protocol, the enrichment step is done at 4 °C with end-over-end rotation (13). The KF does not have a cooling unit and cannot rotate plates end-over-end. Therefore we sought to confirm whether the enrichment step should be performed offline at 4 °C as is done in the manual protocol or on the KF at RT with mixing. To evaluate the capture step, two 96-well KF plates were prepared, each with three wells containing 500  $\mu$ g Jurkat peptides and the HS mag anti-K- $\epsilon$ -GG.

One 96-well plate was rotated end-over-end in a cold room at 4 °C, and the other plate was incubated on the KF at room temperature with mixing set to “medium” (supplemental Fig. S3B and supplemental Data S4). A large drop in PSMs was observed when the incubation was performed at RT on the KingFisher, identifying 3308 K- $\epsilon$ -GG PSMs compared with 6215 K- $\epsilon$ -GG PSMs with end-over-end rotation at 4 °C. These results indicate that offline end-over-end rotation at 4 °C is required to maximize binding of K- $\epsilon$ -GG peptides to the anti-K- $\epsilon$ -GG antibody. Performing this step offline does not add any additional time or labor since the samples and beads are already in the 96-well plate; however, future studies could explore placing the KingFisher in a cold room at 4 °C.

Next we determined the optimal amount of HS mag anti-K- $\epsilon$ -GG beads for K- $\epsilon$ -GG peptide enrichment on the KF. Previous work showed that decreasing the amount of agarose-bead anti-K- $\epsilon$ -GG antibody increased the relative yield and overall recovery of K- $\epsilon$ -GG peptides, presumably by reducing nonspecific binding of unmodified peptides (13). Given the previous findings, we titrated the amount of HS mag anti-K- $\epsilon$ -GG to determine which bead volume would produce the highest overall number and the highest relative yield of K- $\epsilon$ -GG peptides using a fixed amount of 500  $\mu$ g of input peptide. We performed quintuplicate enrichments using 5  $\mu$ l, 10  $\mu$ l, and 20  $\mu$ l of HS mag anti-K- $\epsilon$ -GG and compared the overall number of K- $\epsilon$ -GG PSMs and relative yield (supplemental Fig. S3C and supplemental Data S5). The number of identified K- $\epsilon$ -GG PSMs was 6519, 5261, and 4540 for 5, 10, and 20  $\mu$ l of HS mag anti-K- $\epsilon$ -GG, respectively. The relative yield of K- $\epsilon$ -GG PSMs was 29%, 23%, and 20% for 5, 10, and 20  $\mu$ l of HS mag anti-K- $\epsilon$ -GG, respectively.

While enrichment with 5  $\mu$ l HS mag anti-K- $\epsilon$ -GG provided the best overall number of K- $\epsilon$ -GG PSMs, the relative yield of K- $\epsilon$ -GG PSMs to total PSMs was much lower for HS mag anti-K- $\epsilon$ -GG processing on the KF relative to manual processing (29% versus 51%). We hypothesized that the decrease in relative yield of K- $\epsilon$ -GG peptides could be due to insufficient bead washing because the volume of each wash step was reduced from 1 ml in the manual protocol to 250  $\mu$ l on the KF to accommodate the maximum volume of the 96-well plate. To reduce the number of non-K- $\epsilon$ -GG peptides resulting from automated processing, 50% ACN was added to the wash buffer to increase stringency. To evaluate the utility of ACN addition to the wash buffer, we performed a label-free experiment where K- $\epsilon$ -GG peptides were enriched from 500  $\mu$ g Jurkat peptides where bead washing was completed with or without 50% ACN added to the HS IAP Wash Buffer (supplemental Fig. S3D and supplemental Data S6). Addition of 50% ACN to the washing buffer increased both the relative yield of K- $\epsilon$ -GG peptides and the absolute number of identified K- $\epsilon$ -GG peptides. An average of 7210 K- $\epsilon$ -GG PSMs with 57% relative yield were identified with 50% ACN added to the wash buffer. In contrast, only 5694 K- $\epsilon$ -GG PSMs with 29% relative yield were identified when ACN was not added. Taken together, we find that use of 5  $\mu$ l of HS

mag anti-K- $\epsilon$ -GG bead slurry and inclusion of 0.01% CHAPS and 50% ACN in wash buffers provide the best performance of the UbiFast method on the KF.

### Manual Versus Automated TMT 10-Plex Experiment

The UbiFast method is designed to be used with multiplexed samples (20). To evaluate the performance of the automated UbiFast workflow, we carried out a head-to-head comparison using HS mag anti-K- $\epsilon$ -GG where both automated and manual UbiFast methods were used to analyze ten process replicates of peptides from Jurkat cells, with 500  $\mu$ g peptide input per replicate using a different TMT10 labeling reagent for each replicate. Due to the additional time it takes to prepare and aliquot TMT reagents in a 96-well plate for multiplexed experiments, we performed two independent automated TMT10 UbiFast experiments comparing 10 min and 20 min on-

antibody TMT labeling time to determine if a longer TMT labeling time is needed due to reagent hydrolysis during preparation steps (Fig. 2A). For manual and automated experiments, we assessed the efficiency of TMT labeling, relative yield of K- $\epsilon$ -GG peptides, and the variability between differentially labeled TMT channels (Fig. 2, B–D, supplemental Data S7).

Using the manual UbiFast protocol, we identified 16,141 distinct K- $\epsilon$ -GG peptides with 97% of peptides being labeled with TMT and a relative yield of 75%. The automated UbiFast experiment identified 21,468 with 88% relative yield and 21,601 distinct K- $\epsilon$ -GG peptides with 87% relative yield using 10 and 20 min of on-antibody TMT labeling time, respectively. Increasing on-antibody TMT labeling time from 10 min to 20 min increased the TMT labeling efficiency from 95% to 97%. The reproducibility of automated UbiFast experiments was higher than manual UbiFast, with median coefficients of

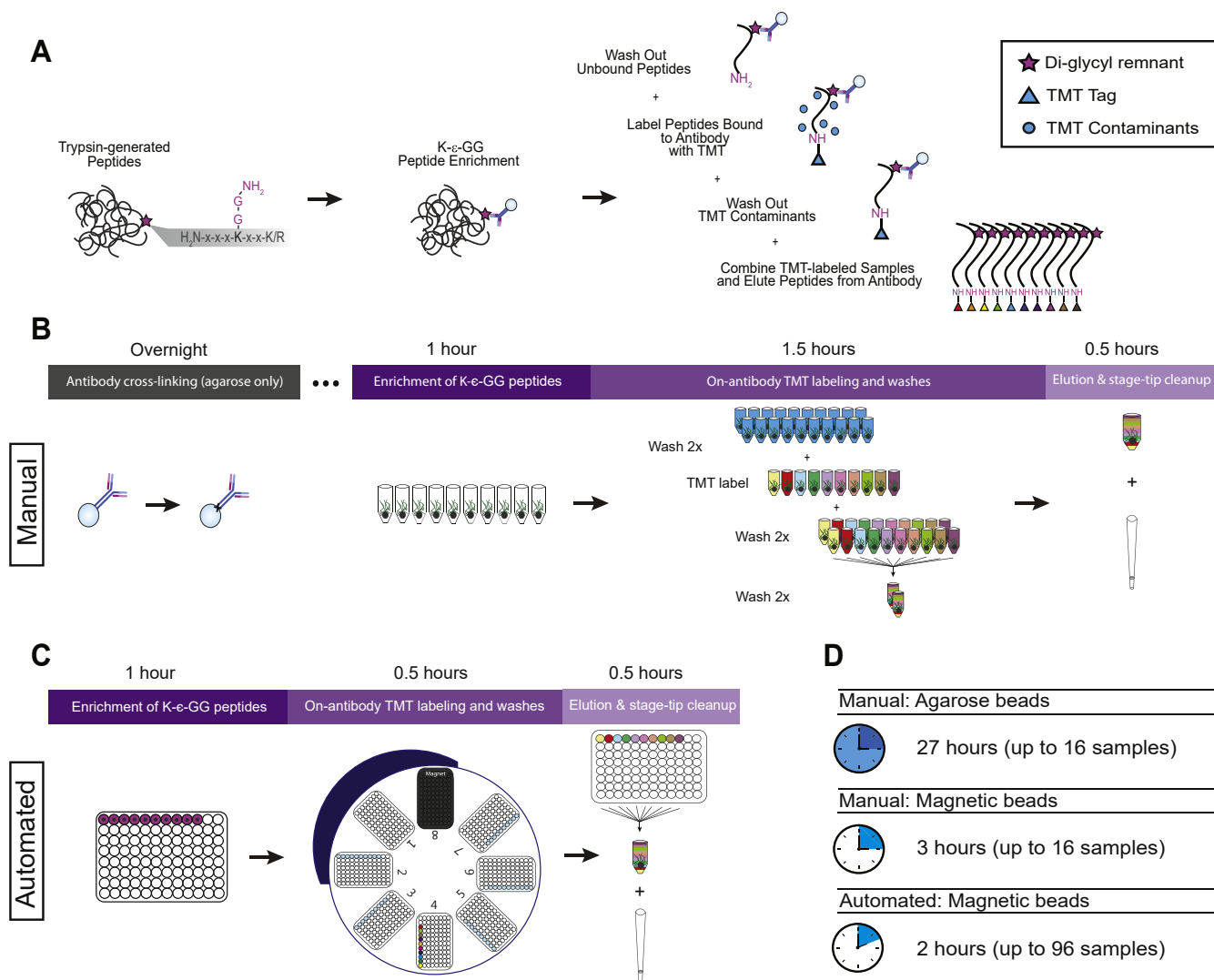
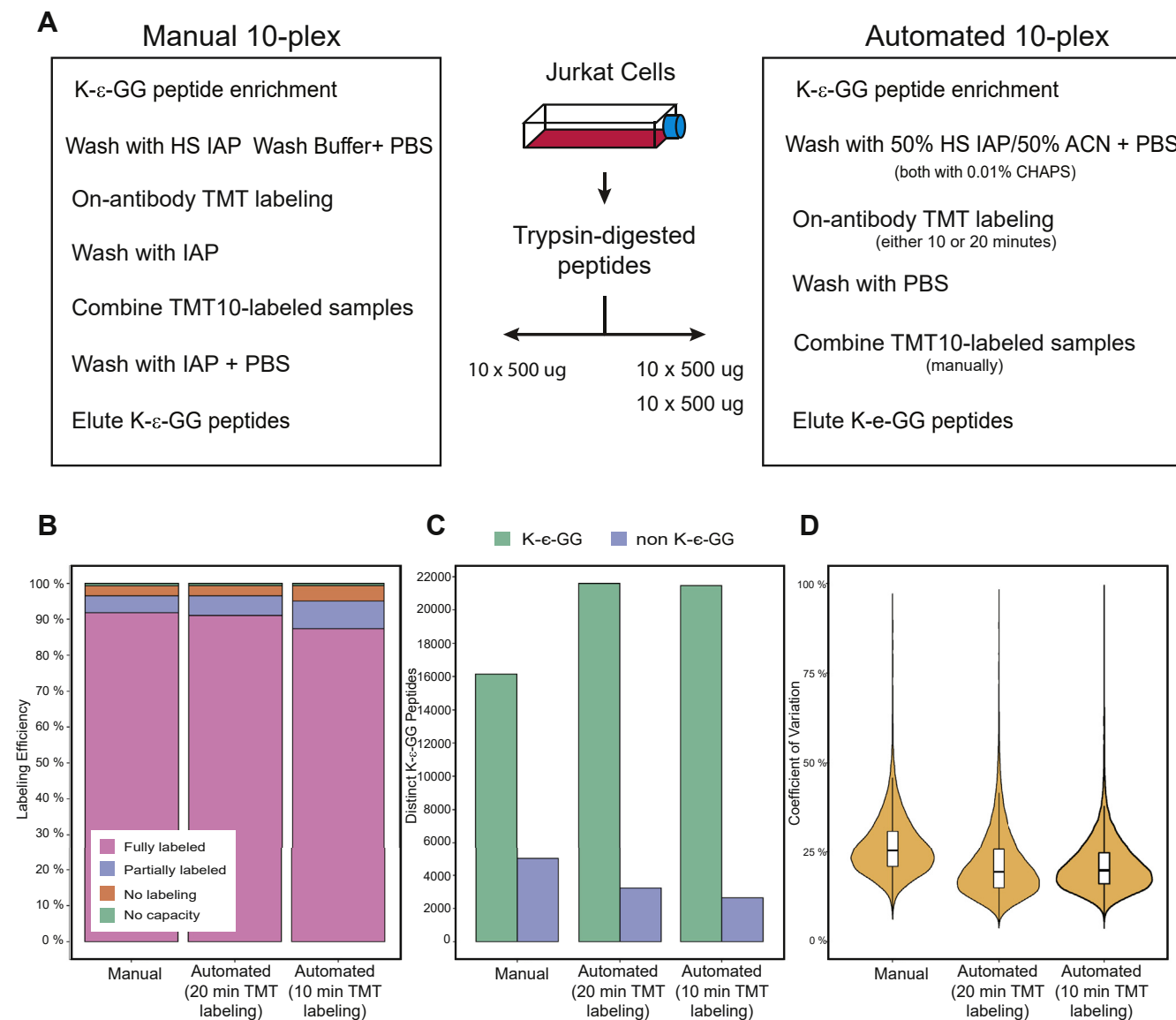


FIG. 1. Comparison of methods for on-antibody labeling of K- $\epsilon$ -GG peptides with isobaric reagents. A, workflow of on-antibody labeling of K- $\epsilon$ -GG peptides with isobaric reagents using the UbiFast method. B, manual UbiFast workflow for processing a TMT10 experiment. C, automated workflow of processing samples for a TMT10 experiment using 96-well plates and a KingFisher Flex instrument.



**FIG. 2. Analysis of K-ε-GG peptide enrichment in a 10-plex format using automation versus manual workflows.** *A*, experimental design of parallel 10-plex ubiquitin enrichment experiments using TMT10 reagents for on-antibody TMT labeling. *B*, stacked bar plots show the percentage of fully, partially and unlabeled K-ε-GG PSM *c* Bar plots of K-ε-GG (green) and non K-ε-GG (blue) distinct peptides identified in each experiment. *D*, violin plots show the distribution of CV's between differentially labeled TMT channels for each experiment with the inner box and whisker plots showing the median and interquartile range.

variation across process replicates of 20%, 19%, 25% for automated UbiFast 10 min, automated UbiFast 20 min, manual UbiFast, respectively. These data indicate that the automated platform washes enriched K-ε-GG peptides and performs on-antibody TMT labeling with high reproducibility, eliminating the need for manual processing.

#### *Performing Multiple Experiments in Parallel Using the Automated UbiFast Method*

Automating the UbiFast method reduces the hands-on time for processing a single multiplexed TMT experiment, but the greatest impact would be in the ability to scale the number of

multiplexed TMT experiments that could be processed simultaneously. To evaluate the effects of processing multiple TMT experiments, we designed an experiment in which 4 × TMT10 experiments were processed in parallel (Fig. 3A). Briefly, a batch of peptides digested with trypsin from A375 cells were aliquoted into 40 × 500 μg aliquots. The 40 aliquots were split into four groups of ten and processed on the KF as described above with each group of ten aliquots processed as separate TMT10 experiments. To assess performance across all four experiments, we evaluated the number of distinct K-ε-GG peptides, the coefficient of variation for each experiment and the labeling efficiency (Fig. 3, B–

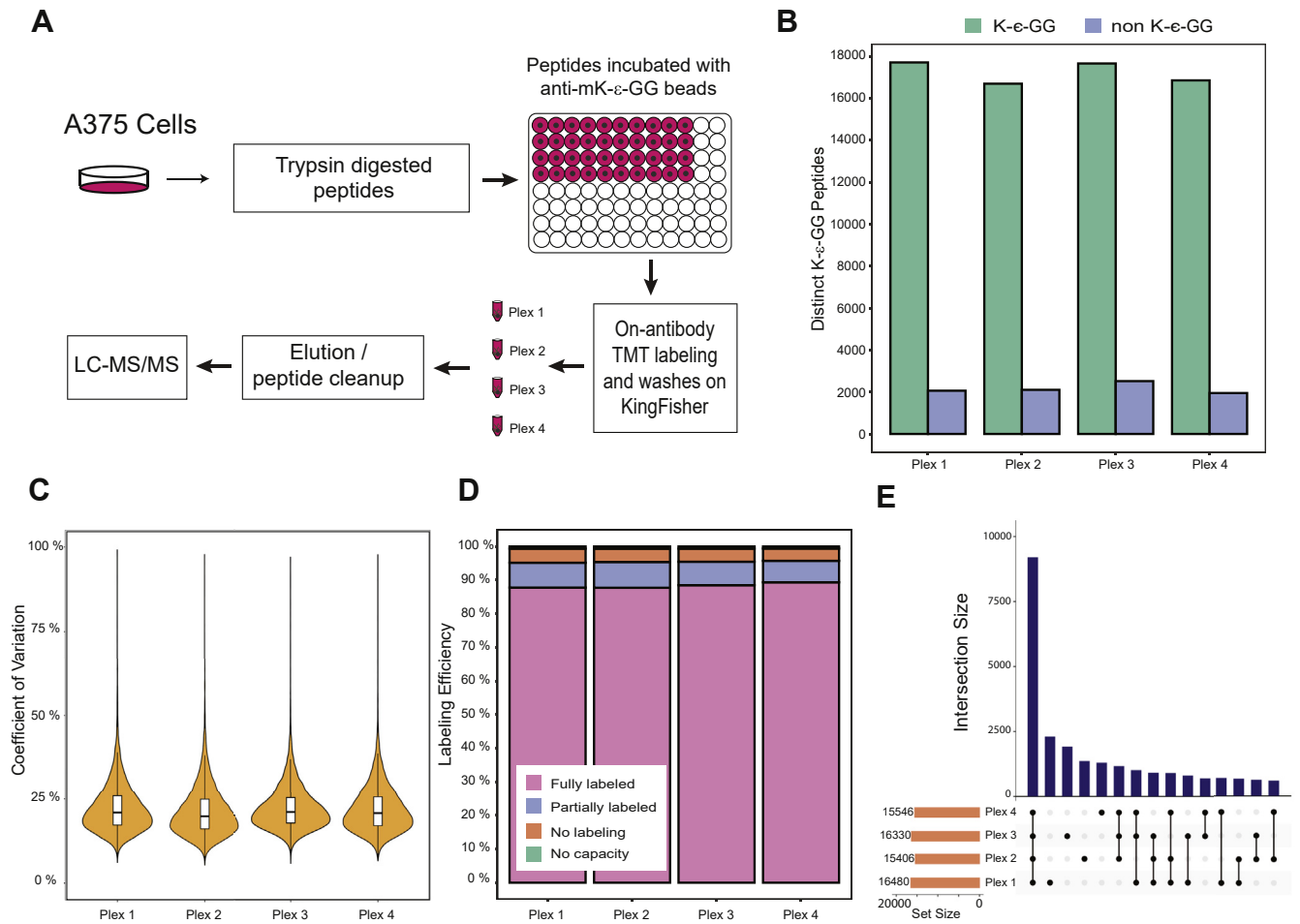


**FIG. 3. Parallel processing of 4 × TMT10 experiments using the automated UbiFast method.** *A*, schematic of experimental workflow for processing multiple experiments in parallel. *B*, stacked bar plots show the percentage of fully, partially and unlabeled K-ε-GG PSMs. *C*, bar plots of K-ε-GG (green) and non K-ε-GG (blue) distinct peptides identified in each experiment. *D*, violin plots show the distribution of CV's between differentially labeled TMT channels for each experiment with the inner box and whisker plots showing the median and interquartile range. *E*, upset plot showing overlap of K-ε-GG sites across experiments run in parallel.

*D* and supplemental Data S8). We identified 17,718, 16,704, 17,668, and 16,862 distinct K-ε-GG peptides in experiments 1 through 4, respectively. The median coefficient of variation for each plex was 20.8, 19.8, 21.2, and 20.8 and the percentage of fully labeled K-ε-GG PSMs was 95%–96% for all four plexes. The overlap in identified K-ε-GG sites across these four experiments was 59% (Fig. 3E), similar to the extent of overlap observed across TMT-plexes for other site-specific posttranslational modifications such as phosphorylation (29). These results indicate that the automated UbiFast protocol enables multiple multiplexed TMT experiments to be processed simultaneously with high reproducibility, saving up to 2 h of laboratory time for each additional TMT experiment.

#### Application of Automated UbiFast with HS Mag Anti-K-ε-GG to Analysis of Tumor Samples

Tumor tissues of two breast cancer PDX models, basal subtype (WHIM2) and luminal subtype (WHIM16), have been

extensively characterized in the proteogenomic space, having been shown to harbor subtype-specific signatures (20, 29, 35). To evaluate the automated UbiFast method for profiling ubiquitylomes of small amounts of tumor tissue, we applied the workflow to enrich ubiquitylated peptides from five replicates each of WHIM2 and WHIM16 using 500 μg of peptide per sample in a TMT10-plex experiment (Fig. 4A). The correlation of replicates within the automated UbiFast dataset employing HS mag anti-K-ε-GG beads was high, with median Pearson correlations of 0.76 and 0.73 for basal and luminal subtypes, respectively (Fig. 4B and supplemental Data S9). In total, 14,211 distinct human K-ε-GG peptides were identified and quantified using this method. Ubiquitylation data was compared with previously published results acquired on the sample PDX models, but employing UbiFast in a manual mode using agarose K-ε-GG antibody to evaluate the overlap of K-ε-GG sites and conservation of canonical biological differences between basal and luminal breast cancer models.

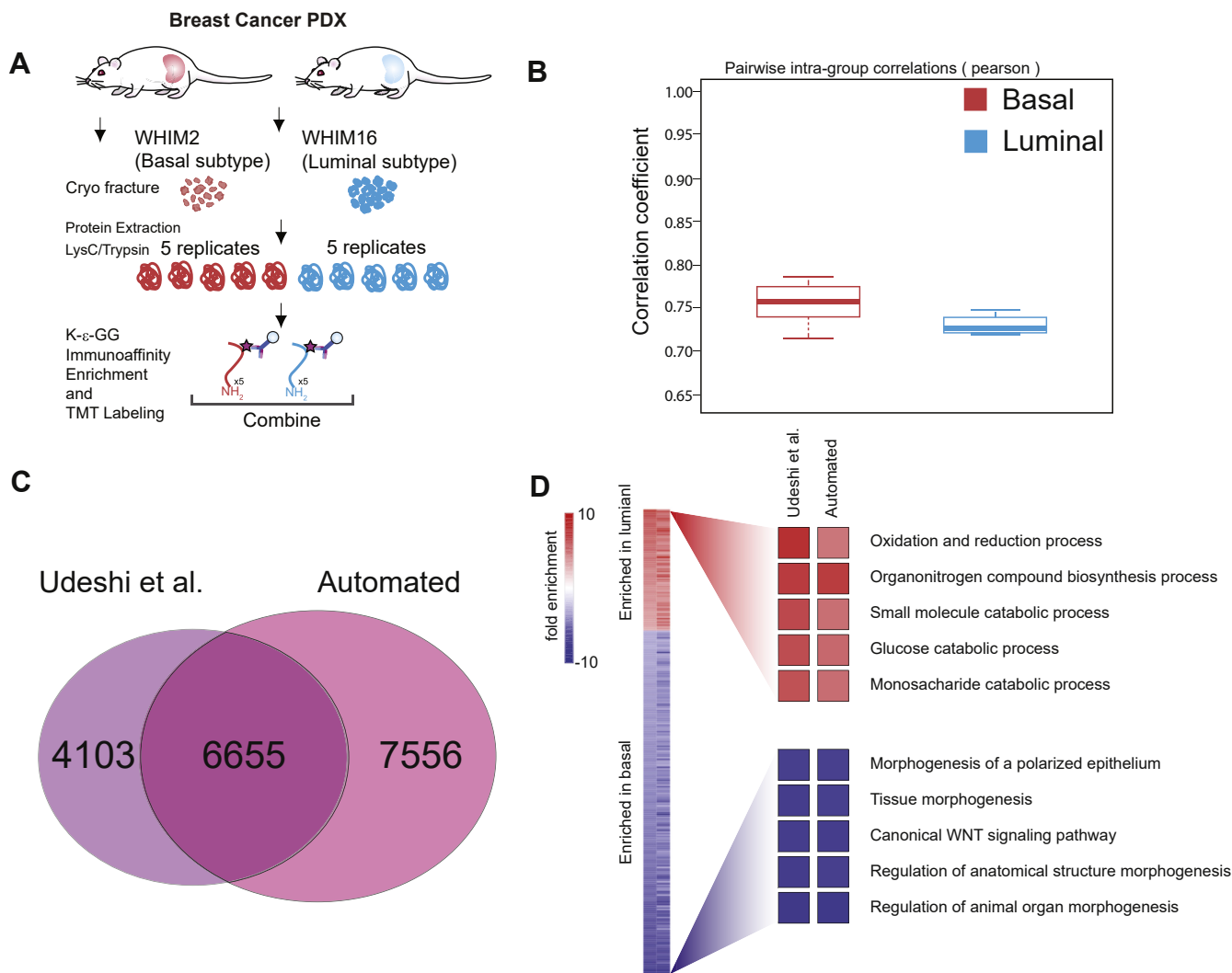


**FIG. 4. Comparison of the ubiquitylomes identified from our automated workflow versus manually workflow (20).** *A*, schematic diagram showing experimental design and process used to enrich K-ε-GG modified peptides from the Luminal and Basal breast cancer PDX models. *B*, Venn Diagram showing overlap of human K-ε-GG sites identified in each dataset. *C*, box of whisker plots of Pearson correlation between replicates of Basal and Luminal PDX models for each dataset. *D*, heatmap of all genesets present in both the Udeshi *et al.* dataset (*left*) and the current, automated dataset (*right*) with the top five most enriched gene sets in the Udeshi *et al.* dataset highlighted.

Among the identified K-ε-GG sites, we see a reasonable degree of overlap at the site level with 61% of sites in the Udeshi *et al.* (20) dataset identified with the automated UbiFast workflow (Fig. 4C). This data is on par with previous studies, which compare overlap of phosphosites within and across laboratories (29). To assess whether biological changes were conserved across UbiFast workflows, we performed gene set enrichment analysis (GSEA) on both datasets using the GO Biological Process Molecular Signature Database (36, 37). Gene Sets that were significantly changing in both datasets are shown in Figure 4D with the top five gene sets enriched in the luminal and basal subtypes from the Udeshi *et al.* study highlighted. It is clear that the gene sets that were significantly enriched with the automated method show the same trends as those enriched by Udeshi *et al.*

## DISCUSSION

Here we present an automated UbiFast workflow using magnetic-bead K-ε-GG antibody and a robotic magnetic particle processor with a 96-well plate format to increase sample analysis throughput of the UbiFast method while decreasing labor required and chances for human error (Fig. 1). Removing the need for a highly trained person to perform these enrichments should make ubiquitylation site profiling accessible to more laboratories. Using the manual implementation of the UbiFast method, it takes more than 1 day of processing time to prepare ten samples (1 × 10-plex experiment) for injection on the mass spectrometer because the antibody must first be cross-linked to agarose beads followed by quality control (29). The antibody supplied in the PTMScan HS Ubiquitin/SUMO Remnant Motif (K-ε-GG) kit is

already linked to the magnetic beads and does not require additional cross-linking, simplifying the method and reducing the total processing time to 3 h per  $1 \times 10$ -plex experiment. Importantly, the magnetic HS mag anti-K- $\epsilon$ -GG reagent identifies many more K- $\epsilon$ -GG peptides with greater reproducibility than the agarose bead anti-K- $\epsilon$ -GG reagent in TMT experiments. We reason that the improvement in the identification of K- $\epsilon$ -GG sites obtained with HS mag bead reagent is due to reduced nonspecific binding to magnetic beads. Additionally, increased reproducibility from automated bead handling on the KF likely results in increasing the number of K- $\epsilon$ -GG peptides identified across all TMT channels.

We demonstrated the importance of titrating the amount of HS mag anti-K- $\epsilon$ -GG reagent antibody used for peptide enrichment to maximize identifications while minimizing the extent of nonspecific peptide enrichment (33, 38). Using more than the optimized amount of antibody defined here results in reduced identification of K- $\epsilon$ -GG peptides likely due to increased nonspecific binding of nonmodified peptides to the antibody.

HS mag anti-K- $\epsilon$ -GG reagent uses the same antibody as is supplied with the agarose bead PTMScan Ubiquitin Remnant Motif (K- $\epsilon$ -GG) Kit (#5562) directly compared to in this study. The key differences between the reagents are the bead type (magnetic *versus* agarose) and the irreversible binding of the anti-K- $\epsilon$ -GG antibody to beads in the case of the HS mag anti-K- $\epsilon$ -GG reagent. Because the antibody itself is the same between the reagents, high-overlap in K- $\epsilon$ -GG peptides identified is expected. In line with this, HS mag anti-K- $\epsilon$ -GG reagent identified 74% of the K- $\epsilon$ -GG peptides identified with agarose anti-K- $\epsilon$ -GG reagent in head-to-head testing experiments shown in [supplemental Figure S1](#).

Automation of the UbiFast method on the KF allows for parallel processing of up to  $9 \times$  TMT10-plex experiments. Automation also reduces variability relative to manual processing methods, with 25% variation observed with manual processing and 19–20% variation with automation. Parallelization of the method significantly increases processing throughput and precision as seen by the average overlap of 59% across parallel experiments (Fig. 3E). Further improvements to the UbiFast workflow that address sensitivity by decreasing the required sample input will likely incorporate low-input proteomic sample processing techniques (39–42). Use of higher-plex isobaric labeling methods such as TMTPro (Thermo Fisher) (17, 18, 19) will enable  $6 \times 16$ -plex or  $5 \times 18$ -plex experiments to be processed in parallel, further increasing sensitivity and throughput. Importantly, the automated UbiFast method is compatible with serial enrichment strategies that enable efficient use of limited amounts of biological and clinical samples (43). Alternate MS data acquisition strategies, such as analysis with a tims-TOF instrument may further improve sensitivity (44). We envision future use of the KF platform to automate the enrichment of other PTMs, such as phosphorylated tyrosine and acetylated lysine as magnetic

bead reagents become available. Finally, HS mag anti-K- $\epsilon$ -GG reagent combined with alternate enzymes like WalP may be used to study protein sumoylation (45).

#### DATA AVAILABILITY

The raw mass spectrometry data have been deposited in the public proteomics repository MassIVE (<http://massive.ucsd.edu>) with the dataset identifier MSV000087363.

*Supplemental data*—This article contains [supplemental data](#).

*Funding and additional information*—This work was supported by the National Cancer Institute (NCI) grants U24CA210986, U01CA214125, and U24CA210979 to S. A. C., Swiss National Science Foundation (SNF) Sinergia grant CRSII5\_186405 to S. A. C., Dr Miriam and Sheldon G. Adelson Medical Research Foundation to S. A. C. and N. D. U. and by a SPARC Award to N. D. U. from the Broad Institute of MIT & Harvard (#800373).

*Author contributions*—K. D. R., M. E. O., S. A. C., and N. D. U. conceptualization; K. A. L. S. S., S. A. C., and N. D. U. data curation; K. D. R., M. E. O., E. J. B., A. J. N., K. A. L., S. S., S. A. C., and N. D. U. formal analysis; K. D. R., M. E. O., and E. J. B. investigation; K. D. R., M. E. O., S. A. C., and N. D. U. writing—original draft.

*Conflict of interest*—S. A. C. is a member of the scientific advisory boards of Kymera, PTM Biolabs, and Seer and an ad hoc scientific advisor to Pfizer and Biogen. All other authors declare no competing interests.

*Abbreviations*—The abbreviations used are: AGC, automatic gain control; Arg, arginine; FDR, false discovery rate; GG, glycine–glycine; HCD, higher-energy collisional dissociation; LC-MS/MS, liquid chromatography–tandem mass spectrometry; Lys, lysine; mK- $\epsilon$ -GG, magnetic bead-conjugated K- $\epsilon$ -GG antibody; PDX, patient-derived xenograft; TFA, trifluoroacetic acid; TMT, tandem mass tag.

Received May 5, 2021, and in revised form, August 23, 2021  
Published, MCPRO Papers in Press, September 27, 2021, <https://doi.org/10.1016/j.mcpro.2021.100154>

#### REFERENCES

- Hershko, A., and Ciechanover, A. (1998) The ubiquitin system. *Annu. Rev. Biochem.* **67**, 425–479
- Buetow, L., and Huang, D. T. (2016) Structural insights into the catalysis and regulation of E3 ubiquitin ligases. *Nat. Rev. Mol. Cell Biol.* **17**, 626–642
- Weissman, A. M., Shabek, N., and Ciechanover, A. (2011) The predator becomes the prey: Regulating the ubiquitin system by ubiquitylation and degradation. *Nat. Rev. Mol. Cell Biol.* **12**, 605–620
- Celebi, G., Kesim, H., Ozer, E., and Kutlu, O. (2020) The effect of dysfunctional ubiquitin enzymes in the pathogenesis of most common diseases. *Int. J. Mol. Sci.* **21**
- Robak, T., Huang, H., Jin, J., Zhu, J., Liu, T., Samoilova, O., Pylypenko, H., Verhoef, G., Sirtanaratkul, N., Osmanov, E., Alexeeva, J., Pereira, J.,

- Drach, J., Mayer, J., Hong, X., *et al.* (2015) Bortezomib-based therapy for newly diagnosed mantle-cell lymphoma. *N. Engl. J. Med.* **372**, 944–953
6. Adams, J. (2004) The development of proteasome inhibitors as anticancer drugs. *Cancer Cell* **5**, 417–421
  7. Kortuem, K. M., and Stewart, A. K. (2013) Carfilzomib. *Blood* **121**, 893–897
  8. Hideshima, T., Richardson, P., Chauhan, D., Palombella, V. J., Elliott, P. J., Adams, J., and Anderson, K. C. (2001) The proteasome inhibitor PS-341 inhibits growth, induces apoptosis, and overcomes drug resistance in human multiple myeloma cells. *Cancer Res.* **61**, 3071–3076
  9. Schapira, M., Calabrese, M. F., Bullock, A. N., and Crews, C. M. (2019) Targeted protein degradation: Expanding the toolbox. *Nat. Rev. Drug Discov.* **18**, 949–963
  10. Akimov, V., Barrio-Hernandez, I., Hansen, S. V. F., Hallenborg, P., Pedersen, A., Bekker-Jensen, D. B., Puglia, M., Christensen, S. D. K., Vanselow, J. T., Nielsen, M. M., Kratchmarova, I., Kelstrup, C. D., Olsen, J. V., and Blagoev, B. (2018) UbiSite approach for comprehensive mapping of lysine and N-terminal ubiquitination sites. *Nat. Struct. Mol. Biol.* **25**, 631–640
  11. Danielsen, J. M. R., Sylvestersen, K. B., Bekker-Jensen, S., Szklarczyk, D., Poulsen, J. W., Horn, H., Jensen, L. J., Mailand, N., and Nielsen, M. L. (2011) Mass spectrometric analysis of lysine ubiquitylation reveals promiscuity at site level. *Mol. Cell. Proteomics* **10**, M110.003590
  12. Kim, W., Bennett, E. J., Huttlin, E. L., Guo, A., Li, J., Possemato, A., Sowa, M. E., Rad, R., Rush, J., Comb, M. J., Harper, J. W., and Gygi, S. P. (2011) Systematic and quantitative assessment of the ubiquitin-modified proteome. *Mol. Cell* **44**, 325–340
  13. Udeshi, N. D., Mertins, P., Svinkina, T., and Carr, S. A. (2013) Large-scale identification of ubiquitination sites by mass spectrometry. *Nat. Protoc.* **8**, 1950–1960
  14. Na, C. H., Jones, D. R., Yang, Y., Wang, X., Xu, Y., and Peng, J. (2012) Synaptic protein ubiquitination in rat brain revealed by antibody-based ubiquitome analysis. *J. Proteome Res.* **11**, 4722–4732
  15. Xu, G., Paige, J. S., and Jaffrey, S. R. (2010) Global analysis of lysine ubiquitination by ubiquitin remnant immunoaffinity profiling. *Nat. Biotechnol.* **28**, 868–873
  16. Thompson, A., Schafer, J., Kuhn, K., Kienle, S., Schwarz, J., Schmidt, G., Neumann, T., and Hamon, C. (2003) Tandem mass tags: A novel quantification strategy for comparative analysis of complex protein mixtures by MS/MS. *Anal. Chem.* **75**, 1895–1904
  17. Thompson, A., Wolmer, N., Koncarevic, S., Selzer, S., Bohm, G., Legner, H., Schmid, P., Kienle, S., Penning, P., Hohle, C., Berfelde, A., Martinez-Pinna, R., Farztdinov, V., Jung, S., Kuhn, K., *et al.* (2019) TMTpro: Design, synthesis, and initial evaluation of a proline-based isobaric 16-plex tandem mass tag reagent set. *Anal. Chem.* **91**, 15941–15950
  18. Li, J., Van Vranken, J. G., Vaites, L. P., Schweppe, D. K., Huttlin, E. L., Etienne, C., Nandhikonda, P., Viner, R., Robitaille, A. M., Thompson, A. H., Kuhn, K., Pike, I., Bomgardner, R. D., Rogers, J. C., Gygi, S. P., *et al.* (2020) TMTpro reagents: A set of isobaric labeling mass tags enables simultaneous proteome-wide measurements across 16 samples. *Nat. Methods* **17**, 399–404
  19. Li, J., Cai, Z., Bomgardner, R. D., Pike, I., Kuhn, K., Rogers, J. C., Roberts, T. M., Gygi, S. P., and Paulo, J. A. (2021) TMTpro-18plex: The expanded and complete set of TMTpro reagents for sample multiplexing. *J. Proteome Res.* **20**, 2964–2972
  20. Udeshi, N. D., Mani, D. C., Satpathy, S., Fereshetian, S., Gasser, J. A., Svinkina, T., Olive, M. E., Ebert, B. L., Mertins, P., and Carr, S. A. (2020) Rapid and deep-scale ubiquitylation profiling for biology and translational research. *Nat. Commun.* **11**
  21. Emanuele, M. J., Elia, A. E. H., Xu, Q., Thoma, C. R., Izhar, L., Leng, Y., Guo, A., Chen, Y., Rush, J., Hsu, P. W., Yen, H. S., and Elledge, S. J. (2011) Global identification of modular Cullin-RING ligase substrates. *Cell* **147**, 459–474
  22. Gendron, J. M., Webb, K., Yang, B., Rising, L., Zuzow, N., and Bennett, E. J. (2016) Using the ubiquitin-modified proteome to monitor distinct and spatially restricted protein homeostasis dysfunction. *Mol. Cell. Proteomics* **15**, 2576–2593
  23. Kronke, J., Udeshi, N. D., Narla, A., Garuman, P., Hurst, S. N., McConkey, M., Svinkina, T., Heckl, D., Comer, E., Li, X., Ciarlo, C., Hartman, E., Munshi, N., Schenone, M., Schreiber, S. L., *et al.* (2014) Lenalidomide causes selective degradation of IKZF1 and IKZF3 in multiple myeloma cells. *Science* **343**, 301–305
  24. Povlsen, L. K., Beli, P., Wagner, S. A., Poulsen, S. L., Sylvestersen, K. B., Poulsen, J. W., Nielsen, M. L., Bekker-Jensen, S., Mailand, N., and Choudhary, C. (2012) Systems-wide analysis of ubiquitylation dynamics reveals a key role for PAF15 ubiquitylation in DNA-damage bypass. *Nat. Cell Biol.* **14**, 1089–1098
  25. Sarraf, S. A., Raman, M., Guarani-Pereira, V., Sowa, M. E., Huttlin, E. L., Gygi, S. P., and Harper, J. W. (2013) Landscape of the PARKIN-dependent ubiquitylome in response to mitochondrial depolarization. *Nature* **496**, 372–376
  26. Satpathy, S., Wagner, S. A., Beli, P., Gupta, R., Kristiansen, T. A., Malinova, D., Francavilla, C., Tolar, P., Bishop, G. A., Hostager, B. S., and Choudhary, C. (2015) Systems-wide analysis of BCR signalosomes and downstream phosphorylation and ubiquitylation. *Mol. Syst. Biol.* **11**, 810
  27. Wagner, S. A., Satpathy, S., Beli, P., and Choudhary, C. (2016) SPATA2 links CYLD to the TNF- $\alpha$  receptor signaling complex and modulates the receptor signaling outcomes. *EMBO J.* **35**, 1868–1884
  28. Rose, C. M., Isasa, M., Ordureau, A., Prado, M. A., Beausoleil, S. A., Jedrychowski, M. P., Finley, D. J., Harper, J. W., and Gygi, S. P. (2016) Highly multiplexed quantitative mass spectrometry analysis of ubiquitylomes. *Cell Syst.* **3**, 395–403.e4
  29. Mertins, P., Tang, L. C., Krug, K., Clark, D. J., Gritsenko, M. A., Chen, L., Clauser, K. R., Clauss, T. R., Shah, P., Gillette, M. A., Petyuk, V. A., Thomas, S. N., Mani, D. R., Mundt, F., Moore, R. J., *et al.* (2018) Reproducible workflow for multiplexed deep-scale proteome and phosphoproteome analysis of tumor tissues by liquid chromatography–mass spectrometry. *Nat. Protoc.* **13**, 1632–1661
  30. Shadforth, I. P., Dunkley, T. P. J., Lilley, K. S., and Bessant, C. (2005) i-Tracker: For quantitative proteomics using iTRAQTM. *BMC Genomics* **6**, 1–6
  31. Benjamini, Y., and Hochberg, Y. (1995) Controlling the false discovery rate: A practical and powerful approach to multiple testing. *J. R. Stat. Soc.* **57**, 289–300
  32. Hansen, F. M., Tanzer, M. C., Bruning, F., Bludau, I., Stafford, C., Schulman, B. A., Robles, M. S., Karayel, O., and Mann, M. (2021) Data-independent acquisition method for ubiquitinome analysis reveals regulation of circadian biology. *Nat. Commun.* **12**, 1–13
  33. Udeshi, N. D., Svinkina, T., Mertins, P., Kuhn, E., Mani, D. R., Qiao, J. W., and Carr, S. A. (2013) Refined preparation and use of anti-diglycine remnant (K- $\epsilon$ -GG) antibody enables routine quantification of 10,000s of ubiquitination sites in single proteomics experiments. *Mol. Cell. Proteomics* **12**, 825–831
  34. Kuhn, E., Whiteaker, J. R., Mani, D. R., Jackson, A. M., Zhao, L., Pope, M. E., Smith, D., Rivera, K. D., Anderson, N. L., Skates, S. J., Pearson, T. W., Paulovich, A. G., and Carr, S. A. (2012) Interlaboratory evaluation of automated, multiplexed peptide immunoaffinity enrichment coupled to multiple reaction monitoring mass spectrometry for quantifying proteins in plasma. *Mol. Cell. Proteomics* **11**, M111 013854
  35. Li, S., Shen, D., Shao, J., Crowder, R., Liu, W., Prat, A., He, X., Liu, S., Hoog, J., Lu, C., Ding, L., Griffith, O. L., Miller, C., Larson, D., Fulton, R. S., *et al.* (2013) Endocrine-therapy-resistant ESR1 variants revealed by genomic characterization of breast-cancer-derived xenografts. *Cell Rep.* **4**, 1116–1130
  36. Subramanian, A., Tamayo, P., Mootha, V. K., Mukherjee, S., Ebert, B. L., Gillette, M. A., Paulovich, A., Pomeroy, S. L., Golub, T. R., Lander, E. S., and Mesirov, J. P. (2005) Gene set enrichment analysis: A knowledge-based approach for interpreting genome-wide expression profiles. *Proc. Natl. Acad. Sci. U. S. A.* **102**, 15545–15550
  37. Mootha, V. K., Lindgren, C. M., Eriksson, K., Subramanian, A., Sihag, S., Lehar, J., Puigserver, P., Carlsson, E., Ridderstrale, M., Laurila, E., Houstis, N., Daly, M. J., Patterson, N., Mesirov, J. P., Golub, T. R., *et al.* (2003) PGC-1 $\alpha$ -responsive genes involved in oxidative phosphorylation are coordinately downregulated in human diabetes. *Nat. Genet.* **34**, 267–273
  38. Svinkina, T., Gu, H., Silva, J. C., Mertins, P., Qiao, J., Fereshetian, S., Jaffe, J. D., Kuhn, E., Udeshi, N. D., and Carr, S. A. (2015) Deep, quantitative coverage of the lysine acetylome using novel anti-acetyl-lysine antibodies and an optimized proteomic workflow. *Mol. Cell. Proteomics* **14**, 2429–2440

39. Yi, L., Tsai, C., Dirice, E., Swensen, A. C., Chen, J., Shi, T., Gritsenko, M. A., Chu, R. K., Piehowski, P. D., Smith, R. D., Rodland, K. D., Atkinson, M. A., Matthews, C. E., Kulkarni, R. N., Liu, T., *et al.* (2019) Boosting to amplify signal with Isobaric Labeling (BASIL) strategy for comprehensive quantitative phosphoproteomic characterization of small populations of cells. *Anal. Chem.* **91**, 5794–5801
40. Myers, S. A., Rhoads, A., Cocco, A. R., Peckner, R., Haber, A. L., Schweitzer, L. D., Krug, K., Mani, D. R., Clauser, K. R., Rozenblatt-Rosen, O., Hacohen, N., Regev, A., and Carr, S. A. (2019) Streamlined protocol for deep proteomic profiling of FAC-sorted cells and its application to freshly isolated murine immune cells. *Mol. Cell. Proteomics* **18**, 995–1009
41. Satpathy, S., Jaehnig, E. J., Krug, K., Kim, B., Saltz, A. B., Chan, D. W., Holloway, K. R., Anurag, M., Huang, C., Singh, P., Gao, A., Namai, N., Dou, Y., Wen, B., Vasaike, S. V., *et al.* (2020) Microscaled proteogenomic methods for precision oncology. *Nat. Commun.* **11**, 532
42. [preprint] Hartlmayr, D., Ctortekca, C., Seth, A., Mendjan, S., Tourniaire, G., and Mechtler, K. (2021) An automated workflow for label-free and multiplexed single cell proteomics sample preparation at unprecedented sensitivity. *bioRxiv*. <https://doi.org/10.1101/2021.04.14.439828>
43. [preprint] Abelin, J. G., Bergstrom, E. J., Taylor, H. B., Rivera, K. D., Klaeger, S., Olive, M. E., Clauser, K. R., White, C. J., Maynard, M., Kane, M. H., Pearce, C., Rachimi, S., Gillette, M. A., Satpathy, S., Udeshi, N. D., *et al.* (2021) MONTE enables serial immunopeptidome, ubiquitylome, proteome, phosphoproteome, acetylome analyses of sample-limited tissues. *bioRxiv*. <https://doi.org/10.1101/2021.06.22.449417>
44. Meier, F., Brunner, A., Koch, S., Koch, H., Lubeck, M., Krause, M., Goedecke, N., Decker, J., Kosinski, T., Park, M. A., Bache, N., Hoerning, O., Cox, J., Rather, O., and Mann, M. (2018) Online parallel accumulation-serial fragmentation (PASEF) with a novel trapped ion mobility mass spectrometer. *Mol. Cell. Proteomics* **17**, 2534–2545
45. Lumpkin, R. J., Gu, H., Zhu, Y., Leonard, M., Ahmad, A. S., Clauser, K. R., Meyer, J. G., Bennet, E. J., and Komives, E. A. (2017) Site-specific identification and quantitation of endogenous SUMO modifications under native conditions. *Nat. Commun.* **8**, 1171